AJNR

Time-Saving 3D MR Imaging Protocols with Millimeter and Submillimeter Isotropic Spatial Resolution for Face and Neck Imaging as Implemented at a Single-Site Major Referral Center

Jeffrey P. Guenette and Lei Qin

AJNR Am J Neuroradiol 2024, 45 (6) 737-742
doi: https://doi.org/10.3174/ajnr.A8184
http://www.ajnr.org/content/45/6/737

Time-Saving 3D MR Imaging Protocols with Millimeter and Submillimeter Isotropic Spatial Resolution for Face and Neck Imaging as Implemented at a Single-Site Major Referral Center

Jeffrey P. Guenette and Lei Qin

ABSTRACT

SUMMARY: MR imaging has become the routine technique for staging nasopharyngeal carcinoma, evaluating perineural tumor spread, and detecting cartilage invasion in laryngeal carcinoma. However, these protocols traditionally require in the range of 25 to 35 minutes of acquisition time. 3D sequences offer the potential advantage of time savings through the acquisition of 1-mm or submillimeter resolution isotropic data followed by multiplanar reformats that require no further imaging time. We have iteratively optimized vendor product 3D T1-weighted MR imaging sequences for morphologic face and neck imaging, reducing the average acquisition time of our 3T protocols by 9 minutes 57 seconds (40.9%) and of our 1.5T protocols by 9 minutes 5 seconds (37.0%), while simultaneously maintaining or improving spatial resolution. This clinical report describes our experience optimizing and implementing commercially available 3D T1-weighted MR imaging pulse sequence protocols for clinical face and neck MR imaging examinations using illustrative cases. We provide protocol details to allow others to replicate our implementations, and we report challenges we faced along with our solutions.

ABBREVIATIONS: ETL = echo-train length; SPACE = sampling perfection with application optimized contrasts by using different flip angle evolution; VIBE = volumetric interpolated breath-hold examination

Development of MR imaging pulse sequences has largely focused on the brain (small body part that can remain motionless), heart (dynamic imaging techniques), and other organ-specific indications. Pulse sequences have not been specifically designed for imaging the intricate structures of the face and neck, where there are also challenges associated with swallowing and breathing motion and acquiring data through the relatively large head to the thin neck to the wide shoulders. Many radiology groups, thus, use pulse sequences designed for the brain, shifting the scan range to the face and adding slices for the neck. These vendor product 2D T1-weighted and 2D T2-weighted sequences typically have 5-mm section thickness and 1-mm section gaps. Cranial nerves, neural foramina, extrinsic tongue muscles, and other small structures are difficult to visualize on these images, restricting the extent to which imaging can impact decisions on clinical management. In centers with subspecialized head and neck radiologists and sufficient MR imaging physicist and/or technologist resources, vendor product protocols are often adapted to generate higher-resolution images, typically along the lines of 3-mm section thickness with no section gap and with in-plane resolution of 0.5–0.7 mm (often in the range of 0.75-mm^3 rectangular voxels). With these improvements, MR imaging has become the routine technique for staging nasopharyngeal carcinoma,[1,2] evaluating perineural tumor spread,[3] and detecting cartilage invasion in laryngeal carcinoma.[4] However, these protocols require in the range of 25 to 35 minutes of acquisition time. Since May 2021, we have intermittently modified, tested, and implemented more rapid face and neck MR imaging protocols while aiming to maintain or improve overall spatial resolution and soft-tissue contrasts.

Given previous successful optimization of 3D steady-state, 3D T2-weighted TSE, and 3D ultrashort echo time sequences for visualization of the cranial nerves,[5-8] we iteratively optimized vendor product 3D T1-weighted MR imaging sequences for morphologic face and neck imaging. To date, we have modified the T1-weighted acquisitions in our general/trans-spatial, nasopharynx/nasal cavity, oropharynx/oral cavity, and sinus MR imaging protocols. Our optimization process was as follows: 1) The MR imaging physicist coauthor adapted a vendor product pulse sequence protocol for 1-mm or submillimeter resolution imaging of the face and neck ROI by adjusting the FOV, matrix, scan volume, TR, TE, flip

Received September 9, 2023; accepted after revision January 26, 2024.

From the Division of Neuroradiology (J.P.G.), Brigham and Women's Hospital, Dana-Farber Cancer Institute, Harvard Medical School, Boston, Massachusetts; and Department of Imaging (L.Q.), Dana-Farber Cancer Institute, Harvard Medical School, Boston, Massachusetts.

This study was funded in part by the Association of University Radiologists GE Radiology Research Academic Fellowship.

Please address correspondence to Jeffrey P. Guenette MD, MPH, Division of Neuroradiology, Brigham and Women's Hospital, 75 Francis St, Boston, MA 02115; e-mail: jpguenette@bwh.harvard.edu

Indicates article with online supplemental data.

http://dx.doi.org/10.3174/ajnr.A8184

FIG 1. Sample 3D T1 VIBE (*A*), 3D T1 SPACE (*B*), and postcontrast 3D T1 VIBE Dixon fat-suppression (*C*) images acquired in the same session on a 3T Magnetom Vida system (Siemens) at the level of the oral cavity, retromolar trigone, and parotid glands in a 44-year-old woman with neck pain show excellent discrimination of soft-tissue structure boundaries with subjectively better soft-tissue contrasts on the SPACE than on VIBE and robust fat suppression on the VIBE Dixon.

angle, bandwidth, and acceleration factors based on past experience. 2) The new sequence protocol was run on a patient in addition to the standard routine protocol at the time. 3) The neuroradiologist coauthor reviewed the images and provided the physicist with constructive criticisms on the subjective quality and the process was repeated,[1] or the neuroradiologist was satisfied with the quality and the sequence protocol was adopted. Using this process, we have reduced the average acquisition time for 1) the 3T general/trans-spatial, nasopharynx/nasal cavity, oropharynx/oral cavity, and sinus MR imaging protocols from 24 minutes 21 seconds to 14 minutes 24 seconds, yielding a 9 minute 57 second (40.9%) time savings on average (range, 6 minutes 23 seconds to 13 minutes 18 seconds, 27.7% to 55.4% time savings) and for 2) the same 1.5T protocols from 24 minutes 33 seconds to 15 minutes 29 seconds, yielding a 9 minute 5 second (37.0%) time savings on average (range, 5 minutes 3 seconds to 13 minutes 46 seconds; 21.7% to 59.3% time savings). The total acquisition time for our face and neck MR imaging protocols is now routinely in the 10- to 17-minute range on 3T systems (Table). We have simultaneously maintained or improved the spatial resolution. For example, we have improved the overall spatial resolution in our oropharynx protocol by 35%, decreasing voxel volume from 0.75 to 0.65 mm^3.

This clinical report describes our experience optimizing and implementing commercially available 3D T1-weighted MR imaging pulse sequence protocols for clinical face and neck MR imaging examinations. We provide protocol details to allow others to replicate our implementations, and we outline challenges we faced along with our solutions.

Case Series

Case 1: 3D T1-Weighted Gradient-Echo, TSE, and Fat-Suppression Techniques. We began by optimizing T1-weighted gradient-recalled echo images, called the volumetric interpolated breath-hold examination (VIBE; Siemens) before T1-weighted TSE sequences were available across our scanners. The soft-tissue contrast on the VIBE images was subjectively considered poor by our neuroradiology faculty relative to the 2D and 3D TSE images, providing less contrast between fat and muscle, while blood vessels also had roughly similar intermediate signal intensity. We, therefore, turned to 3D T1-weighted TSE sequences as they became available across our fleet of scanners. We used the Sampling Perfection with Application-optimized Contrasts by using different flip angle Evolution (SPACE sequence; Siemens) and the Cube sequence (GE Healthcare). Our optimization work has been performed with the SPACE sequence on 3T systems, then applied to the Cube sequence, and then adapted for 1.5T systems. Direct comparisons of T1-weighted VIBE and SPACE images are provided for a 44-year-old woman with neck pain in Fig 1.

For postcontrast imaging, the opportunity to acquire both T1-weighted in-phase images and fat-suppressed images in the same acquisition is highly appealing. The fat-suppression technique described by Dixon,[9] in 1984, includes a single-sequence acquisition of both in-phase and opposed-phase data, allowing mathematic processing into 4 contrasts: T1-weighted in-phase, T1-weighted opposed-phase, T1-weighted water, and T1-weighted fat. The implementation of Dixon with a 3D spoiled gradient-echo sequence on Siemens systems is called VIBE Dixon, and on GE Healthcare systems, it is called liver acquisition with volume acceleration flex (LAVA Flex). Anecdotally, we have found the Dixon technique to be more robust than the spectral fat-suppression techniques we use in 2D imaging. Direct comparison of the T1-weighted VIBE Dixon fat-suppressed images is provided in Fig 1 in conjunction with the T1-weighted precontrast images from the same patient.

All our optimized 3D T1-weighted protocol parameters are provided in the Online Supplemental Data to allow replication at other institutions. Information on our optimized 2D T1-weighted protocols and detailed protocol parameters is provided in the Online Supplemental Data.

Case 2: Whole-Neck Protocol and Early Protocol Iteration Showing an Invasive Cutaneous Lesion. For the nonfocal whole-neck protocol, we acquired data in the sagittal plane, which minimizes the scan range and eliminates the potential for wrap artifacts from the body and vertex scalp. Given that this protocol is used

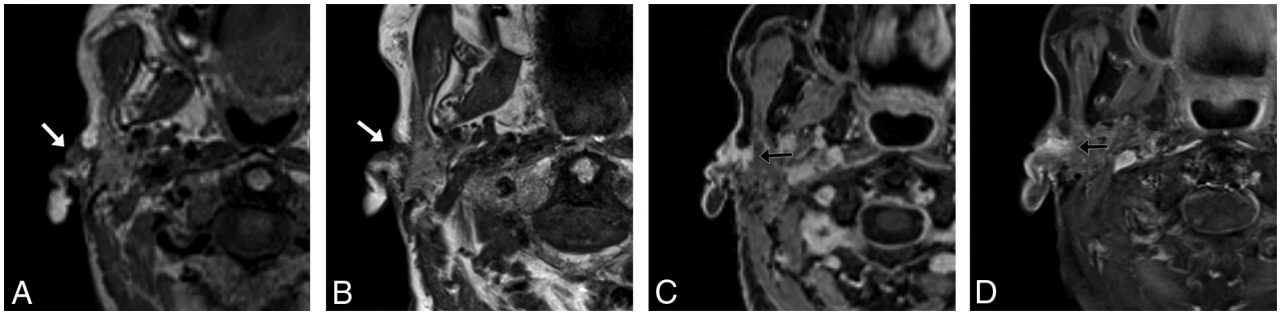

FIG 2. A 92-year-old woman with squamous cell carcinoma. *A*, T1 SPACE sequence performed in the full-neck MR imaging protocol with 2.7-mm^3 (1.4 mm isotropic) voxels during early optimization iterations reformatted into the axial plane clearly shows a cutaneous preauricular lesion (*arrow*) that is not visible due to volume averaging on the 2D T1-weighted image (*B*) with 1-mm^3 (4 × 0.5× 0.5 mm) voxels. The T1 VIBE Dixon (*C*) reformatted image in the axial plane shows the associated infiltrating tumor into the parotid gland (*arrow*) to advantage compared with the 2D T1-weighted image (*D*) with spectral fat suppression. The case convinced us that the SPACE sequence was a reasonable alternative to the 2D standard-of-care and led us to improve the spatial resolution of the SPACE sequence. These images were obtained contemporaneously on a 3T Magnetom Vida system.

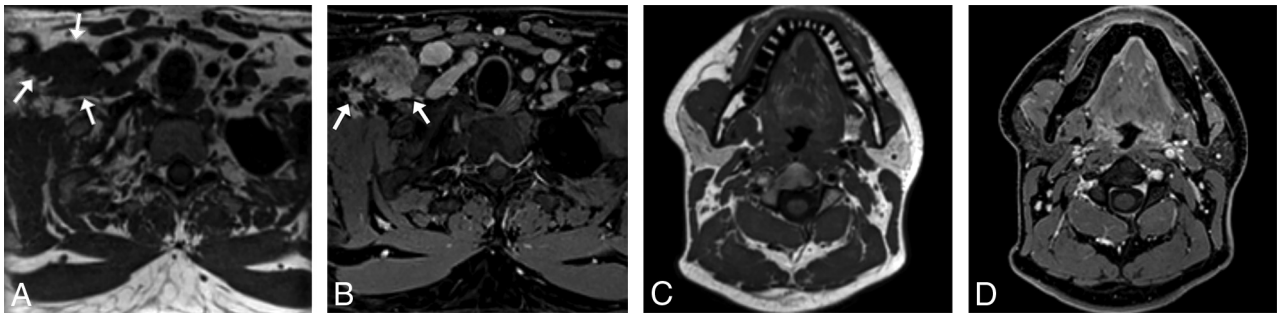

FIG 3. A 27-year-old man with right supraclavicular and chest wall desmoid tumor images on a 1.5T Magnetom Aera system (Siemens). The tumor (*arrows*) is shown on a general neck protocol, 1.0-mm isotropic sagittal acquisition T1 SPACE axial reformat (*A*) and T1 VIBE Dixon (*B*) postcontrast axial reformatted images. Image quality and fat suppression remain good at the level of the thoracic inlet. In addition, T1 SPACE axial reformat (*C*) and T1 VIBE Dixon (*D*) postcontrast axial reformat images through the face are provided to show image quality in that region.

Gradient time savings from MR imaging protocols on 3T Magnetom Prisma and 1.5T Magnetom Aera systems for reference

Protocol	2D T1 Version	3D T1 Version	Time Savings	Savings
3T general	23:05	16:42	6:23	27.7%
3T nasopharynx	23:42	13:38	10:04	42.5%
3T oropharynx	26:37	16:33	10:04	37.8%
3T sinus	24:00	10:42	13:18	55.4%
Mean	24:21	14:24	9:57	40.9%
1.5T general	23:15	18:12	5:03	21.7%
1.5T nasopharynx	24:11	15:26	8:45	36.2%
1.5T oropharynx	27:33	18:48	8:45	31.8%
1.5T sinus	23:14	9:28	13:46	59.3%
Mean	24:33	15:29	9:05	37.0%

Note:—Times listed as minutes:seconds.

for identification of gross soft-tissue abnormalities without the necessity for finer spatial detail, we acquired it at 1-mm isotropic resolution. However, even with 1-mm^3 voxels, this sequence can often more clearly show smaller lesions than in what we traditionally called high-resolution 2D acquisition images, which were submillimeter in-plane but with 3-mm or thicker section thickness. An example is provided in Fig 2 of images from a 92-year-old woman with a small focal preauricular metastasis of cutaneous squamous cell carcinoma invading the parotid gland.

Case 3: One-Millimeter Sagittal Isotropic Whole-Neck Protocol with 1.5T Adaptation. Our 1.5T protocol was adapted from the 3T protocol to provide the same resolution; 1.5T protocol parameters are provided in the Online Supplemental Data alongside the 3T protocol parameters. An example is provided in Fig 3, images from a 27-year-old man with a right supraclavicular and chest wall desmoid tumor.

Case 4: Submillimeter Axial Isotropic Focused Face Protocol. For the higher-resolution targeted 3D T1-weighted protocols, we acquired data in the axial plane to minimize the scan range and allow higher-resolution imaging (0.9 × 0.9 × 0.8 mm) in shorter scan times. This approach requires oversampling to avoid wrap artifacts. However, even with oversampling and the somewhat longer acquisition time compared with the axial 2D protocol, we achieved considerable time savings due to submillimeter near-isotropic voxels, allowing multiplanar reconstructions and eliminating multiple-plane acquisitions (Table). We minimized axial-acquisition time- and phase-encoding steps using a left-right phase-encoding direction and a rectangular FOV. Reformatting images into the coronal and sagittal planes provided us with 3 planes of T1-weighted imaging through the ROI. Furthermore, individual radiologists can adjust the isotropic image planes in our PACS viewer to optimize viewing. To give a rough

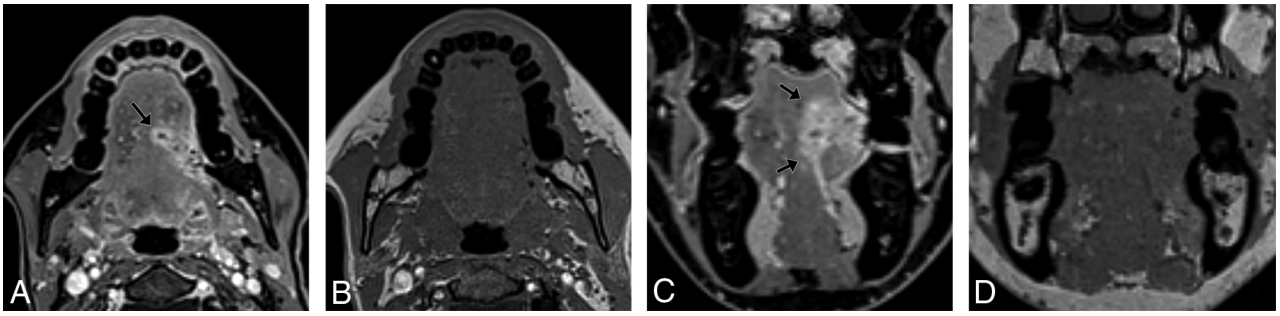

FIG 4. A 44-year-old woman with newly diagnosed oral cavity squamous cell carcinoma (*arrows*) shown on oropharynx protocol T1 VIBE Dixon 0.8 × 0.9 × 0.9 mm resolution axial acquisition (*A*) and coronal reformat images (*B*) and a corresponding precontrast T1 SPACE axial acquisition (*C*) and coronal reformat images (*D*) obtained on a 3T Magnetom Vida system.

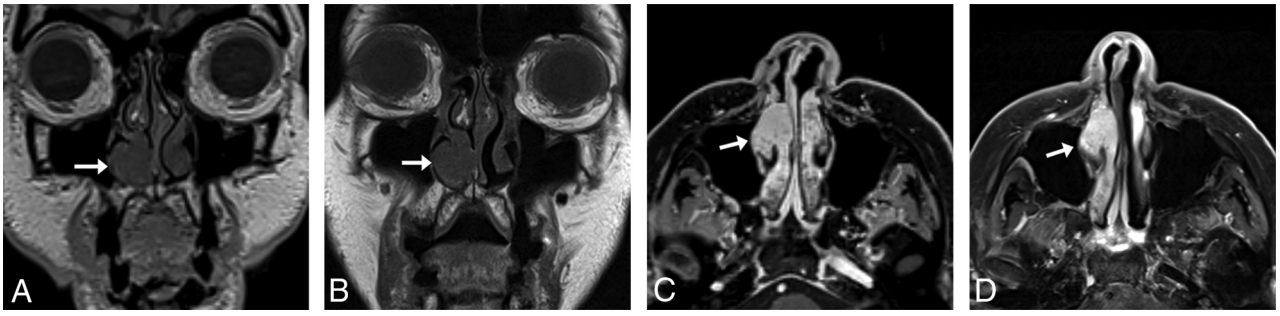

FIG 5. An 83-year-old woman with melanoma and a stable untreated nasal cavity mass of unknown pathology with sinus protocol MR imaging. T1 SPACE coronal acquisition (*A*) performed with 1-mm^3 (1.0 mm isotropic) voxels shows a mass (*arrow*) along the anterior aspect of the right inferior turbinate, seen similarly on the 2D T1-weighted image (*B*) with 0.8-mm^3 (3 × 0.5 × 0.52 mm) voxels. The T1 VIBE Dixon axial reformat (*C*) shows the mass (*arrow*) to advantage compared with the 2D T1-weighted image (*D*) with spectral fat suppression; the former shows the extent of the mass relative to the more heterogeneously enhancing turbinate. The 3D images were acquired on a 3T Magnetom Vida system 6 months following the acquisition of the 2D images on a 3T Magnetom Skyra system (Siemens).

comparison of visual contrast of the 3D images relative to the 2D images of our prior protocol, we measured the signal intensity ratio in 3 consecutive patients who had imaging with the 3D protocol in mid-July of 2023 and who had prior imaging with the 2D protocol also on a 3T MR imaging scanner. In this sample, the lateral pterygoid muscle to retroantral fat mean signal intensity ratio (visual contrast) is similar at 0.41 (SD, 0.05) for this 3D protocol compared with 0.35 (SD, 0.06) for the 2D protocol.

For postcontrast T1-weighted images, we also acquired data in the axial plane at 0.9-mm isotropic resolution with a left-right phase-encoding direction and a rectangular FOV to minimize acquisition time. We have compared anterior-posterior and left-right phase-encoding directions and observed no substantial flow artifacts on images using either encoding direction. In the same sample of 3 consecutive patients, the mean retroantral fat-to-lateral pterygoid muscle signal intensity ratio (visual contrast) was 0.83 (SD, 0.07) for this 3D protocol versus 0.38 (SD, 0.13) for the 2D protocol for examinations performed at different timepoints; there is greater muscle-fat contrast for the 3D than for 2D images.

We show images for this protocol from a 44-year-old woman with newly diagnosed oral cavity squamous cell carcinoma in Fig 4.

Case 5: One-Millimeter Coronal Isotropic Sinus Protocol Showing a Nasal Cavity Mass. For sinus imaging, we acquired data in the coronal plane, from the tip of the nose to the vertebral bodies, to minimize the scan range and scan times. We show sample images of this protocol compared with 2D images for an 83-year-old woman with a stable untreated nasal cavity mass of unknown pathology in Fig 5.

Case 6: Submillimeter Coronal Isotropic Sinus Protocol Showing Perineural Tumor. During our optimization phase, we tested submillimeter coronal acquisitions in our sinus protocol, similar to our high-resolution axial protocol for the nasopharynx and oropharynx. We show an example of perineural tumor from one of these examinations in an 85-year-old man with a spindle cell sarcoma in Fig 6.

DISCUSSION

In this clinical report, we show that it is feasible to leverage commercially available 3D T1-weighted MR imaging pulse sequence protocols to substantially reduce the scan time for clinical face and neck MR imaging examinations while preserving overall spatial resolution and perhaps improving diagnostic quality. We also describe our experience optimizing these sequences and provide protocol parameter details so that others can replicate our implementations.

For quality assurance, our neuroradiologists were asked by group e-mail and in division staff meetings to send negative, positive, and constructive feedback on the diagnostic quality of these images throughout and following the protocol-optimization

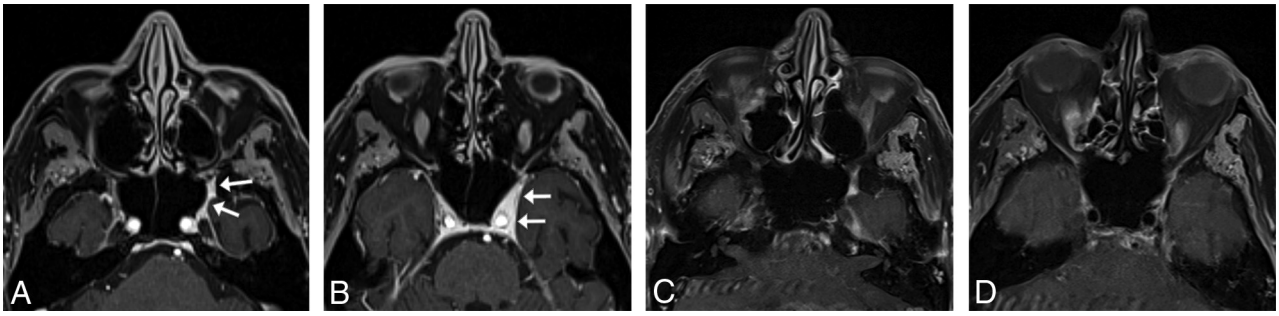

FIG 6. An 85-year-old man with spindle cell sarcoma with sinus protocol MR imaging. T1 VIBE Dixon axial acquisition performed with 0.9-mm^3 (0.74 mm isotropic) voxels clearly shows tumor (*arrows*) along the left V2 (*A*) and in the left lateral cavernous sinus wall (*B*), neither of which is clearly seen on the 2D T1-weighted images (*C* and *D*) with spectral fat suppression with 2-mm^3 (4 × 0.7 × 0.7 mm) voxels. The 3D examination shown was performed on a 3T Magnetom Prisma Fit system (Siemens) 3 weeks before the 2D examination, which was performed on a Siemens 3T Vida system, with no intervening treatment.

process via our department's critical results, peer review, and quality-assurance closed-loop communication tool.[10] We also welcomed and encouraged informal feedback. All feedback requests were open-ended. The group initially provided primarily informal mixed feedback on the quality and appropriateness of the 3D acquisition images. The feedback was always preference-based; we identified no cases in which diagnostic information was obtained on the 2D images but not the 3D images (though we did identify the converse, as shown in Figs 3, 4, and 6). In addition, we initially ran the 3D protocols alongside the 2D protocols. At that time, we were working with the 3D gradient-recalled echo T1-weighted sequence. We gradually phased out the 2D-acquisition images on one of our scanners and then on several additional scanners. We did not introduce the 3D TSE T1-weighted protocol until after the 2D protocols were phased out; thus, we do not have any same-patient same-examination comparisons of 3D TSE T1-weighted images and 2D TSE T1-weighted images for quantitative SNR and contrast-to-noise ratio comparisons. Because our neuroradiologists have become accustomed to the qualitative appearance of the 3D protocol images, we have had no further negative feedback.

The primary technical frustration we have encountered is that while 3D protocols can be set to automatically generate multiplanar reformats on the scanner on Siemens systems, this reformatting mechanism reformats only the in-phase VIBE Dixon images and cannot be modified to select the fat-suppression images for automatic reformatting. We, therefore, rely on a combination of manual reformatting by the technologists at the scanner and on-the-fly reformatting by the radiologists when reviewing images in our PACS system, which has an excellent 3D multiplanar reformatting tool.

On the positive side, not only can shortening acquisition times help reduce motion artifacts, lessen concern for claustrophobia, and increase throughput, it can also provide time to add other useful sequences. In our case, given increasing evidence for DWI utility in head and neck imaging,[11,12] we have been able to add DWI back to our face and neck MR imaging protocols. Time constraints, a focus on high-resolution morphologic imaging, and poor-quality DWI led to removal of DWI from our protocols several years ago. We are also excited to test quantitative arterial spin-labeling and dynamic contrast-enhancement perfusion imaging,[13-16] both of which show considerable promise for diagnostic utility but add acquisition time. Also exciting but currently investigative is the potential for 3D synthetic MR imaging techniques, such as multiplanar multiecho imaging,[17,18] that allow acquisition of all contrasts simultaneously and that could allow mathematic derivation and generation of novel contrasts tailored to face and neck applications.

We report only on T1-weighted imaging protocols because we have not successfully implemented 3D T2 techniques with fat suppression. We have attempted to image with 3D T2 STIR techniques, but the fat suppression consistently fails in the region of the nape of the neck. We hypothesize that this failure is related to the section thickness we tried to achieve and the signal decrease due to the much longer echo-train length (ETL) for 3D (attempted ETL = 150 to keep the scan time within 6 minutes) than 2D STIR (ETL =31), despite our efforts to set a similar effective TE for both 3D and 2D STIR. Furthermore, due to the extended ETL in 3D, the acquired echoes can contain signals from recovered fat, resulting in inadequate fat suppression. Vendor product 3D T2-weighted protocols with Dixon-type fat suppression are not currently available.

We may be able to further reduce acquisition times as we explore deep learning reconstruction capabilities on commercially available vendor upgrades. Optimization of 3D T2-weighted imaging with some form of fat suppression would help further reduce scan times and provide 3-plane T2-weighted images for easy cross-referencing. It may also be worth exploring T1-weighted ultrashort echo time sequences, given the ability to visualize bone and cranial nerves on these images.[6,19] For now, the optimized commercially available 3D T1-weighted protocols have substantially improved our clinical face and neck MR imaging examination workflows and also anecdotally appear to have had a positive impact on our diagnostic capabilities.

In summary, our experience shows that it is feasible to leverage commercially available 3D T1-weighted MR imaging pulse sequence protocols to substantially reduce the scan time for clinical face and neck MR imaging examinations while preserving overall spatial resolution and perhaps improving diagnostic quality.

Disclosure forms provided by the authors are available with the full text and PDF of this article at www.ajnr.org.

REFERENCES

1. Razek AA, King A. **MRI and CT of nasopharyngeal carcinoma.** *AJR Am J Roentgenol* 2012;198:11–18 CrossRef Medline
2. Chong VF, Fan YF. **Skull base erosion in nasopharyngeal carcinoma: detection by CT and MRI.** *Clin Radiol* 1996;51:625–31 CrossRef Medline
3. Moonis G, Cunnane MB, Emerick K, et al. **Patterns of perineural tumor spread in head and neck cancer.** *Magn Reson Imaging Clin N Am* 2012;20:435–46 CrossRef Medline
4. Cho SJ, Lee JH, Suh CH, et al. **Comparison of diagnostic performance between CT and MRI for detection of cartilage invasion for primary tumor staging in patients with laryngo-hypopharyngeal cancer: a systematic review and meta-analysis.** *Eur Radiol* 2020;30:3803–12 CrossRef Medline
5. Guenette JP, Ben-Shlomo N, Jayender J, et al. **MR imaging of the extracranial facial nerve with the CISS sequence.** *AJNR Am J Neuroradiol* 2019;40:1954–59 CrossRef Medline
6. Guenette JP, Seethamraju RT, Jayender J, et al. **MR imaging of the facial nerve through the temporal bone at 3T with a noncontrast ultrashort echo time sequence.** *AJNR Am J Neuroradiol* 2018;39:1903–06 CrossRef Medline
7. Casselman JW, Kuhweide R, Deimling M, et al. **Constructive interference in steady state-3DFT MR imaging of the inner ear and cerebellopontine angle.** *AJNR Am J Neuroradiol* 1993;14:47–57 Medline
8. Alkan A, Sigirci A, Ozveren MF, et al. **The cisternal segment of the abducens nerve in man: three-dimensional MR imaging.** *Eur J Radiol* 2004;51:218–22 CrossRef Medline
9. Dixon WT. **Simple proton spectroscopic imaging.** *Radiology* 1984;153:189–94 CrossRef Medline
10. Glazer DI, Zhao AH, Lacson R, et al. **Use of a PACS embedded system for communicating radiologist to technologist learning opportunities and patient callbacks.** *Curr Probl Diagn Radiol* 2022;51:511–16 CrossRef Medline
11. Miracle AC, El-Sayed IH, Glastonbury CM. **Diffusion weighted imaging of esthesioneuroblastoma: differentiation from other sinonasal masses.** *Head Neck* 2019;41:1161–64 CrossRef Medline
12. Yeom KW, Lober RM, Mobley BC, et al. **Diffusion-weighted MRI: distinction of skull base chordoma from chondrosarcoma.** *AJNR Am J Neuroradiol* 2013;34:1056–61, S1 CrossRef Medline
13. Amukotuwa SA, Marks MP, Zaharchuk G, et al. **Arterial spin-labeling improves detection of intracranial dural arteriovenous fistulas with MRI.** *AJNR Am J Neuroradiol* 2018;39:669–77 CrossRef Medline
14. Sun Z, Hu S, Ge Y, et al. **Can arterial spin labeling perfusion imaging be used to differentiate nasopharyngeal carcinoma from nasopharyngeal lymphoma?** *J Magn Reson Imaging* 2021;53:1140–48 CrossRef Medline
15. Baba A, Kurokawa R, Rawie E, et al. **Normalized parameters of dynamic contrast-enhanced perfusion MRI and DWI-ADC for differentiation between posttreatment changes and recurrence in head and neck cancer.** *AJNR Am J Neuroradiol* 2022;43:1184–89 CrossRef Medline
16. Ota Y, Liao E, Capizzano AA, et al. **Diagnostic role of diffusion-weighted and dynamic contrast-enhanced perfusion MR imaging in paragangliomas and schwannomas in the head and neck.** *AJNR Am J Neuroradiol* 2021;42:1839–46 Medline
17. Cheng CC, Preiswerk F, Hoge WS, et al. **Multipathway multi-echo (MPME) imaging: all main MR parameters mapped based on a single 3D scan.** *Magn Reson Med* 2019;81:1699–713 CrossRef Medline
18. Cheng CC, Preiswerk F, Madore B. **Multi-pathway multi-echo acquisition and neural contrast translation to generate a variety of quantitative and qualitative image contrasts.** *Magn Reson Med* 2020;83:2310–21 CrossRef Medline
19. Bracher AK, Hofmann C, Bornstedt A, et al. **Ultrashort echo time (UTE) MRI for the assessment of caries lesions.** *Dentomaxillofac Radiol* 2013;42:20120321 CrossRef Medline